Eur Radiol (2011) 21:850–856
DOI 10.1007/s00330-010-1974-5

UROGENITAL

Differentiation of benign and malignant uterine corpus tumors by using proton MR spectroscopy at 3T: preliminary study

Mayumi Takeuchi · Kenji Matsuzaki · Masafumi Harada

Received: 30 May 2010 / Revised: 20 August 2010 / Accepted: 25 August 2010 / Published online: 3 October 2010

Abstract
Objective To retrospectively evaluate the diagnostic ability of magnetic resonance (MR) spectroscopy for distinguishing benign and malignant lesions in patients with uterine corpus tumours at MR imaging.
Methods Pelvic MR spectroscopy was performed in patients with pathologically diagnosed benign and malignant uterine corpus tumours at 3T-MR imaging. Single-voxel MR spectroscopy data were collected from a single square volume of interest that encompassed the uterine corpus lesion. The total choline compounds (tCho) resonance peak areas were quantified relative to unsuppressed water using a software package. Patients who fulfilled the criteria for estimates of acceptable reliability were included.
Results A total of 32 patients (age range, 24–76 years) with 32 lesions were evaluated in this study. The median lesion size at MR imaging was 50 mm (range, 19–218 mm). A tCho peak was present in all 32 lesions including 14 malignant lesions (9.21±2.21 mM), and 18 benign lesions (4.59±2.22 mM) ($p<0.0001$). Using a cut-off value of 7.00 mM for malignant lesions had a sensitivity of 93%, specificity of 83%, PPV of 81% and NPV of 94%.
Conclusion Proton MR spectroscopy with quantitative evaluation of tCho concentration can provide helpful information in distinguishing benign and malignant uterine corpus tumours.

M. Takeuchi (✉) · K. Matsuzaki
Department of Radiology, University of Tokushima,
3-18-15, Kuramoto-cho,
zip:7708503 Tokushima, Japan
e-mail: mayumi@clin.med.tokushima-u.ac.jp

M. Harada
Department of Medical Imaging, University of Tokushima,
Tokushima, Japan

Keywords MRI · MR spectroscopy · Uterine corpus tumour · Choline-containing compounds · Quantitative evaluation

Introduction

Both benign and malignant processes can occur within the endometrial cavity; therefore, preoperative diagnosis is important to plan treatment. Various benign and malignant tumours in the endometrial cavity, such as endometrial polyp, endometrial hyperplasia and endometrial cancer may show similar magnetic resonance (MR) manifestations [1–3]. However some diseases can be diagnosed via endometrial cytology or endometrial curettage, conclusive pathological diagnosis is not always available. The treatment needed for benign endometrial polyp or hyperplasia is polypectomy and curettage, whereas the standard treatment of endometrial carcinoma is hysterectomy with bilateral salpingo-oophorectomy [4, 5]. On the other hand, most of the uterine myometrial tumours are benign leiomyomas, typically appearing as well-circumscribed low signal intensity masses on T2-weighted images [6]. However, it may occasionally be difficult to distinguish leiomyomas from malignant tumours because leiomyomas may show high signal intensity on T2-weighted images because of oedema or degeneration [7–9]. Benign leiomyomas are usually asymptomatic and not require treatment. When leiomyomas are symptomatic, interfere with fertility, or show rapid growth, hormonal therapy or surgical treatment such as myomectomy or hysterectomy may be required [10]. Because malignant myometrial tumours usually require surgical treatment as soon as possible, diagnosis based on imaging is important. Both malignant uterine corpus tumours and benign lesions with cystic components, oedema or degeneration show high

signal intensity on T2-weighted images, it may be difficult to distinguish malignant and benign uterine corpus lesions by conventional MR imaging [5–7]. Proton MR spectroscopy (hydrogen 1 [1H] MR spectroscopy) provides metabolic information, which is useful for the differentiation of benign and malignant tumours in the brain, prostate and other various organs [11–16]. The diagnostic value of proton MR spectroscopy is typically based on the detection of elevated levels of total choline compounds (tCho) such as choline, phosphocholine and glycerophosphocholine, which are biomarkers of cancer tissue and are increased in actively proliferating tumours [17, 18]. 3T-MRI can offer high-quality MR spectroscopy because of superior spectral separation and increased signal-to-noise ratio. The purpose of this study is to verify the feasibility of MR spectroscopy at 3T to differentiate benign and malignant uterine corpus tumours.

Materials and methods

Patients

Our institutional review board approved this retrospective study and informed consent was obtained from each patient before performance of MR spectroscopy. We cross-referenced the gynaecological database of our institution to identify all patients who had undergone MR spectroscopy for the evaluation of uterine corpus tumours between April 2007 and August 2009. Forty-three patients with uterine corpus tumours had undergone MR spectroscopy. Of these 43 patients, those who fulfilled the following three criteria were retrospectively included in the study: known histological diagnosis made by surgical resection, dilatation and curettage, or transvaginal biopsy; lesions containing enough solid components for MR spectroscopic measurement; the tCho concentration with a percentage standard deviation (%SD) <20%. That was because %SD <20% has been used by many as a criterion for estimates of acceptable reliability according to the LCModel manual [19]. The data of eleven of the 43 patients were excluded from the study because histological diagnosis was not available in seven patients, three lesions contained minimal solid components because of massive necrosis, and %SD >20% in one patient. The data of 32 patients who had a total of 32 uterine corpus tumours and fulfilled these criteria were included in the study: 32 women with a mean age of 54 years (range, 24–76 years). The 32 uterine corpus tumours included 14 malignant tumours (11 endometrial carcinomas and 3 myometrial tumours: one rhabdomyosarcoma and 2 malignant lymphoma) and 18 benign tumours (5 endometrial polyps/hyperplasia and 13 myometrial lesions: 11 leiomyomas and 2 adenomyotic lesions). The median lesion size, which was the longest diameter measured by MR imaging was 50 mm (range, 19–218 mm).

MR Spectroscopic measurement

All patients were studied on 3T superconducting MRS using body coil transmission and an 8-channel phased-array receiver designed for cardiac studies (Signa HDx 3T, GE Healthcare, Milwaukee, WI, USA). T2-weighted axial fast spin echo images (512×288 over a 28-cm field of view; 6-mm section thickness with a 1-mm intersection gap; repetition time/echo time, 7000/100 milliseconds), and diffusion-weighted axial echo planar images (128×192 over a 40-cm field of view; 5-8-mm section thickness with a 0-2-mm intersection gap; repetition time/echo time, 6000–6500/56.1–64 milliseconds; *b* factors, 0 and 800 s/mm^2) were obtained to depict the anatomy. The b value was set at 800 s/mm^2, high enough to reduce the effects of perfusion of the tissue and T2 shine-through effect, and low enough to maintain the signals of background structures for image interpretation. Using these images, a single square spectroscopic volume-of-interest (VOI) was prescribed within the uterine corpus tumours, avoiding cystic or necrotic areas as possible for heterogeneous lesions. The voxel size was 8 mL (2×2×2 cm^3), and outer volume suppression bands were automatically applied at the six edges of the VOI. However the size of VOI may cause the restriction of measurement in smaller tumours, the size was not reduced to maintain the detectability of metabolites. All patients were studied using point resolved spectroscopic sequence (PRESS) sequence (repetition time/echo time, 2000/144 milliseconds) with an automated shimming method. The number of averages was 96 for the acquisition with water suppression and 12 for unsuppressed water spectrum, and total MR spectroscopic data acquisition took about 5 min.

Analysis methods

The presence of tCho peak at 3.2 ppm was visually evaluated at first by two radiologists (K. M. and M. T.) with 20 and 11 years' experience in pelvic MR imaging, respectively. They were blinded to the histopathological and clinical diagnoses of the lesions. The metabolite concentration level was classified into three classes, in comparison with the noise level by visual estimation: that is, twofold higher than the average noise level (++), higher than the average noise level but lower than a twofold higher noise level (+), and the same as the average noise level (–) [20, 21]. Agreement between the two radiologists was reached in consensus after careful individual evaluation. Signals in spectra were analysed by LCModel (version 6.2, Stephen Provencher Inc.) and the quantification of the tCho level was based on the unsuppressed water reference signal

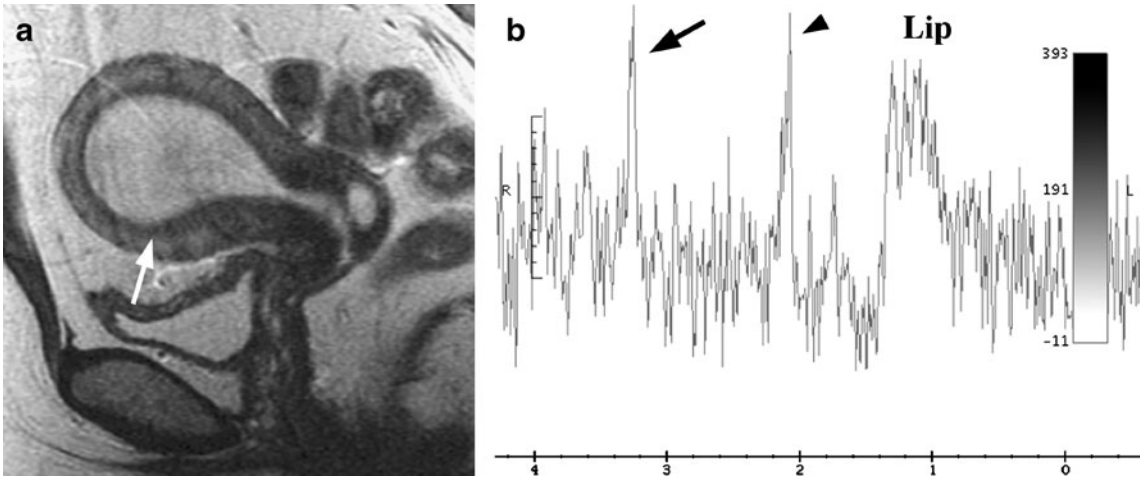

Fig. 1 A 58-year-old woman with an endometrial polyp. **a**. Sagittal T2-weighted fast spin-echo image (TR/TE, 7000/106.7) shows hyper-intense mass (*arrow*) in the uterine cavity. **b**. Single-voxel MR spectroscopy image shows a low tCho peak (*arrow*) with an estimated tCho concentration of 1.98 mM. A low peak (*arrowhead*) at 2-2.1 ppm may be assigned to N-acethyl mucous compounds. Lip: Lipid peak centred at 1.3 ppm

together with the assumed water concentration obtained from the same voxel using the automated water-scaling function in the LCModel package. The tCho ratio to the unsuppressed water was converted to approximate mM units assuming the concentration of MR-visible tissue water content to be 35 M [22]. The criteria for selecting reliable metabolite concentrations were based on the %SD of the fit for each metabolite reflecting the Cramer-Rao lower bounds. Only results with a %SD <20% were included in the analysis [19]. The Mann-Whitney U test was used to compare the tCho concentration among benign and malignant uterine corpus tumours. A value of $p<0.05$ was considered statistically significant. The tCho concentration cut-off value (mM) to differentiate benign from malignant lesions was calculated, with their sensitivity, specificity, positive predictive value (PPV) and negative predictive value (NPV).

Results

The tCho peak was observed in all 32 uterine corpus tumours (Figs. 1, 2, 3, and 4). Six benign lesions were classified as (+), and the other 12 benign lesions and all 14 malignant lesions were classified as (++). The tCho concentration in malignant tumours (9.21±2.21 mM) was significantly higher than that in benign lesions (4.59±2.22 mM) ($p<0.0001$) (Fig. 5). The average full-width at half-maximum was 7.2± 3.0 Hz. There was no significant difference between the tCho concentration in malignant endometrial and myometrial

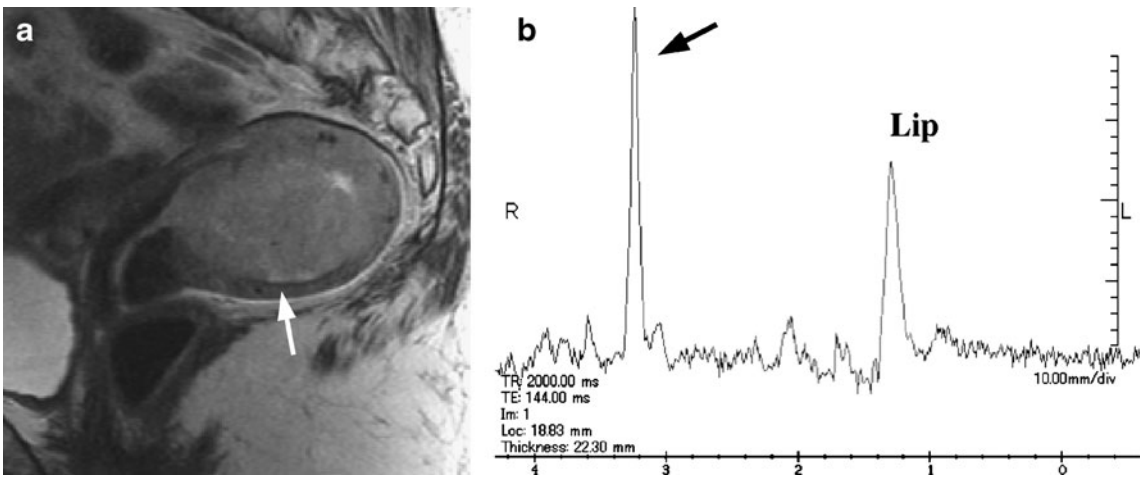

Fig. 2 A 66-year-old woman with endometrial cancer (serous adenocarcinoma). **a**. Sagittal T2-weighted fast spin-echo image (TR/TE, 7000/106.7) shows a hyper-intense mass (*arrow*) in the uterine cavity. **b**. Single-voxel MR spectroscopy image shows a high tCho peak (*arrow*) with an estimated tCho concentration of 10.70 mM. Lip: Lipid peak centred at 1.3 ppm

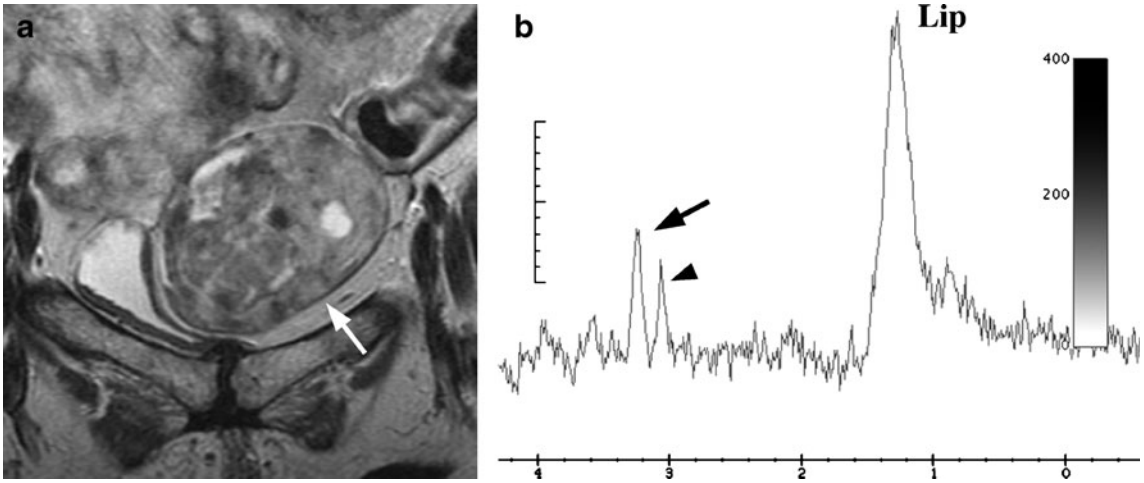

Fig. 3 A 61-year-old woman with uterine leiomyoma with oedematous change. **a**. Coronal T2-weighted fast spin-echo image (TR/TE, 7000/105.6) shows a heterogeneously hyper-intense uterine myometrial mass (*arrow*). **b**. Single-voxel MR spectroscopy image shows a low tCho peak (*arrow*) with an estimated tCho concentration of 4.80 mM. A low creatine peak (*arrowhead*) at 3 ppm is observed. Lip: Lipid peak centred at 1.3 ppm

tumours (p=0.10), and in benign endometrial and myometrial lesions (p=0.17) (Fig. 6). Using a cut-off value of 7.00 mM for overall malignant tumours had a sensitivity of 93% (13/14), specificity of 83% (15/18), PPV of 81% (13/16) and NPV of 94% (15/16). Using a cut-off value of 7.00 mM for endometrial malignant tumours had a sensitivity of 91% (10/11), specificity of 100% (5/5), PPV of 100% (10/10) and NPV of 83% (5/6), and for myometrial malignant tumours had a sensitivity of 100% (3/3), specificity of 77% (10/13), PPV of 50% (3/6) and NPV of 100% (10/10). Only one malignant lesion (endometrial cancer, well differentiated endometrioid carcinoma, grade 1, stage Ia; size: 40 mm) showed a tCho concentration lower than 7.00 mM (4.35 mM), whereas three benign lesions (leiomyomas including one cellular leiomyoma; size 64, 96, and 116 mm) showed a tCho concentration higher than 7.00 mM (7.76 to 8.44 mM). The endometrial cancer with low tCho concentration was diagnosed as low-grade endometrioid carcinoma and no obvious necrosis was revealed on histopathological examination. The leiomyomas with high tCho concentration were relatively larger lesions occurred in younger patients (32–42 years old). No marked degeneration was observed in these lesions on histopathological examination. Although some benign myometrial lesions such as leiomyomas with oedema or myxoid degeneration and adenomyotic lesions showed heterogeneous high signal intensity on T2-weighted images mimicking uterine sarcomas, low tCho concentration suggested their benignity (Fig. 3).

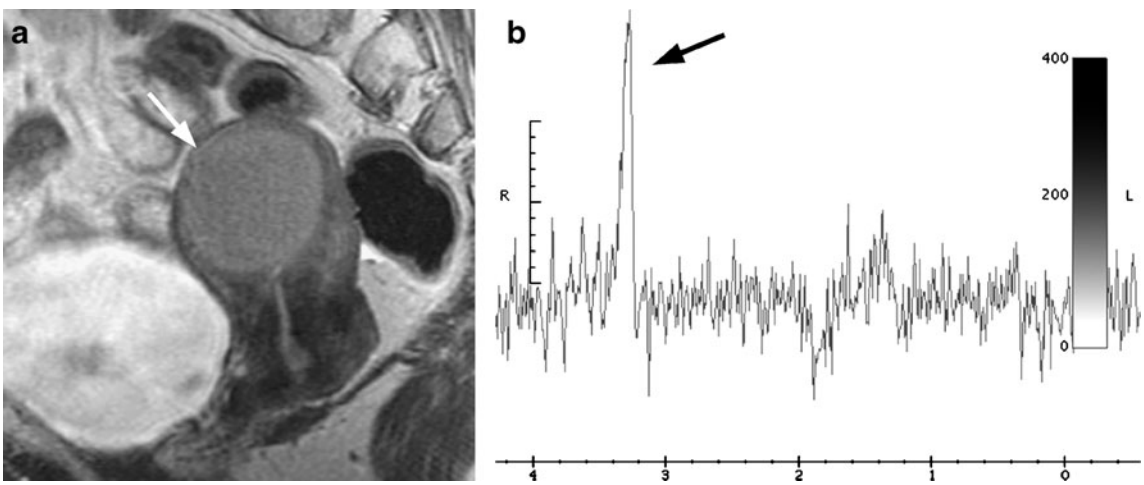

Fig. 4 A 62-year-old woman with a malignant lymphoma. **a**. Sagittal T2-weighted fast spin-echo image (TR/TE, 7000/106.7) shows a hyper-intense uterine myometrial mass (*arrow*). **b**. Single-voxel MR spectroscopy image shows a high tCho peak (*arrow*) with an estimated tCho concentration of 8.49 mM

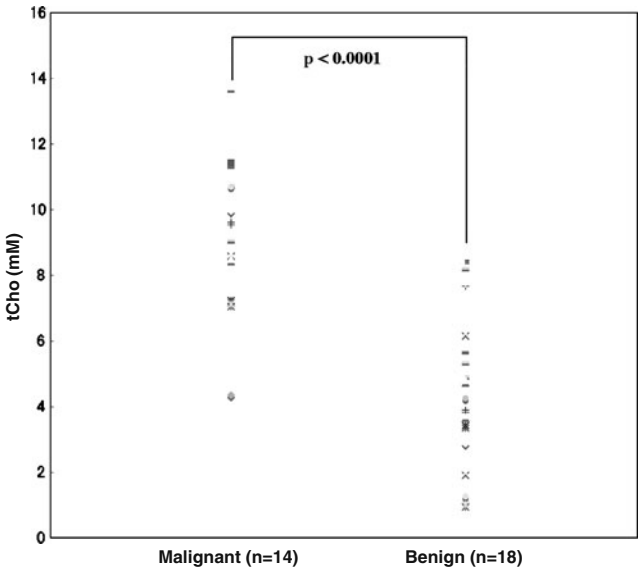

Fig. 5 Scatter plots of the tCho concentration obtained in benign and malignant uterine corpus tumours. The tCho concentration in malignant lesions is significantly higher than that in benign lesions ($p<0.0001$)

Discussion

In our study the tCho peak was observed in all solid tumours, and tended to show a higher peak in malignancy by visual evaluation. These observations are consistent with previous MR spectroscopic studies in various gynaecological abnormalities [20–25]. Okada et al. performed MR spectroscopy at 1.5T and found tCho peak in the solid portion of all benign and malignant female intrapelvic tumours (ovarian tumours including ovarian cancer and thecoma, uterine lesions including endometrial carcinoma, leiomyoma, adenomyosis and intrapelvic neurogenic tumours), and the signal intensity varied among different histological types of tumours possibly reflecting the metabolic activity of the cell membrane [20, 26]. The qualitative analysis of tCho is not discriminating enough to differentiate benign and malignant lesions.

By their semiquantified evaluation of tCho concentration both benign uterine lesions (leiomyomas and adenomyosis) and uterine malignancy (endometrial carcinoma) were classified as (++). They concluded that the tCho could not be used for differential diagnosis between benign and malignant tumours [20]. In our results all malignant lesions were classified as (++), whereas one-third of benign lesions were classified as (+) and the other two-thirds were as (++). Although malignant tumours tended to show a higher tCho peak, there was considerable overlap.

Celik et al. performed MR spectroscopy at 1.5T and found the tCho peak in 14 of the 15 leiomyomas [21]. In their results six leiomyomas were classified as (+) and eight were as (++) by the same semiquantified evaluation methods as Okada's and ours [20, 21]. Booth et al. performed MR spectroscopy at 3T and have found tCho peak in a high proportion of all their gynaecological neoplasms, both benign and malignant, (ovarian cancer, and uterine tumours including endometrial and cervical cancers and leiomyoma) [24]. Visually assessed higher levels of tCho in malignant tumours compared with the benign lesions may be due to the enhancement of phospholipid basement membrane turnover associated with tumour cell proliferation [24, 26]. However, quantification of the tCho concentration is recommended to improve

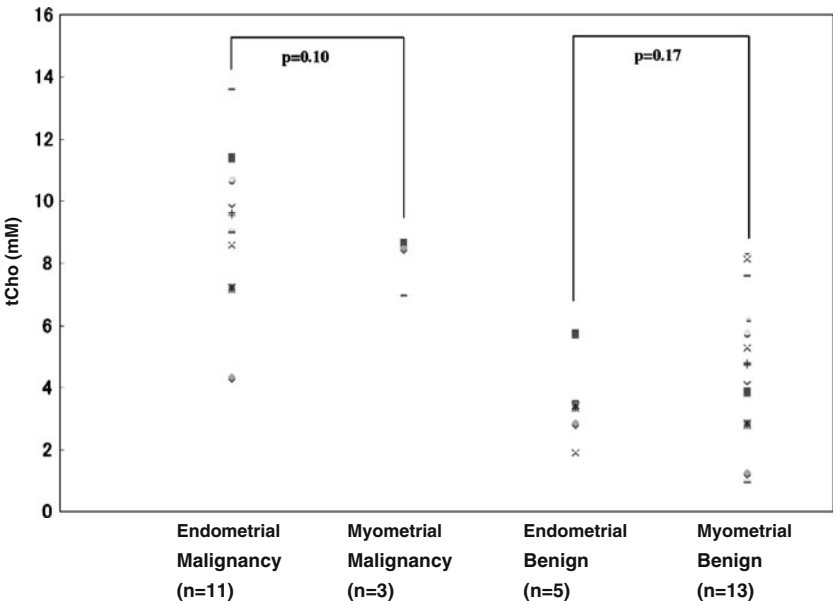

Fig. 6 Scatter plots of the tCho concentration obtained in malignant endometrial and myometrial tumours, and in benign endometrial and myometrial lesions. There are no significant differences between the tCho concentration in malignant endometrial and myometrial tumours ($p=0.10$), and in benign endometrial and myometrial lesions ($p=0.17$)

diagnostic accuracy by determining objective detection thresholds, inter-observer reproducibility and ease of inter-patient comparison [22].

Stanwell et al. performed semi-quantitative analysis of ovarian tumours at 3T by calculating the ratio of choline/creatine (Cho/Cr) for each voxel studied [25]. Because creatine peak is generally much smaller than choline peak, the creatine ratio method may magnify experimental errors [22].

On the other hand, the internal water signal is very intense and this approach has been pursued in several studies [16, 18, 22]. McLean et al. applied LCModel to quantify the tCho concentration relative to water in evaluating ovarian tumours [22, 27, 28]. In our study the tCho concentration in malignant tumours was 9.21± 2.21 mM, and similar ranges in tCho (water-normalised tCho varied 2.0–16.6 mM) were reported by McLean et al. in primary and metastatic ovarian cancers obtained at 3T [22]. They found that MR spectroscopy of ovarian masses could be measured at 3T with acceptable spectral quality and good signal-to-noise ratio for semi-quantitative or quantitative analysis of metabolites [22, 25].

Ours is the first study to attempt to differentiate benign and malignant uterine corpus tumours by using MR spectroscopy at 3T with quantification of the tCho concentration. Both benign endometrial polyps/hyperplasia and endometrial cancer, and both malignant myometrial tumours and some benign myometrial lesions with oedema or myxoid degeneration showed high signal intensity on T2-weighted images, and quantitative evaluation of the tCho concentration was helpful to distinguish between benign and malignant tumours. Because VOI was prescribed within the tumours, avoiding cystic or necrotic areas as possible in our study, the tCho concentration was considered to correlate with the biochemical activity of solid tumoural viable components, and was higher in malignant tumours [26]. The retrospective nature of the study and the relatively small population were limitations of our study. In addition, histologically unproven cases were excluded from this study. Prospective studies with larger populations are needed to support our results. Recently the usefulness of diffusion-weighted MR imaging in diagnosing gynecologic diseases was reported in several studies [9, 29–32]. Malignant uterine corpus tumours show high signal intensity on diffusion-weighted imaging reflecting hypercellularity of tumour cells and long T2 relaxation time of cancerous tissues [9, 30–32]. Malignant tumours with increased cellularity show low apparent diffusion coefficient (ADC) values, whereas relative hypocellular benign lesions tend to show relatively higher ADC values [9, 30–32]. The comparative study of MR spectroscopy and diffusion-weighted imaging may be required to improve the overall diagnostic ability of MRI. We conclude that MR spectroscopy with quantitative evaluation of the tCho concentration can provide helpful information in distinguishing benign and malignant uterine corpus tumours.

References

1. Grasel RP, Outwater EK, Siegelman ES, Capuzzi D, Parker L, Hussain SM (2000) Endometrial polyps: MR imaging features and distinction from endometrial carcinoma. Radiology 214:47–52
2. Nalaboff KM, Pellerito JS, Ben-Levi E (2001) Imaging the endometrium: disease and normal variants. Radiographics 21:1409–1424
3. Takeuchi M, Matsuzaki K, Uehara H, Yoshida S, Nishitani H, Shimazu H (2005) Pathologies of the uterine endometrial cavity: usual and unusual manifestations and pitfalls on magnetic resonance imaging. Eur Radiol 15:2244–2255
4. Kurman RJ, Mazur MT (1994) Benign diseases of the endometrium. In: Kurman RJ (ed) Blaustein's pathology of the female genital tract, 4th edn. New York, Springer-Verlag, pp 367–409
5. Kurman RJ, Zaino RJ, Norris HJ (1994) Endometrial carcinoma. In: Kurman RJ (ed) Blaustein's pathology of the female genital tract, 4th edn. New York, Springer-Verlag, pp 439–486
6. Hricak H, Tscholakoff D, Heinrichs L, Fisher MR, Dooms GC, Reinhold C, Jaffe RB (1986) Uterine leiomyomas: correlation of MR, histopathologic findings, and symptoms. Radiology 158:385–391
7. Ueda H, Togashi K, Konishi I, Kataoka ML, Koyama T, Fujiwara T, Kobayashi H, Fujii S, Konishi J (1999) Unusual appearances of uterine leiomyomas: MR imaging findings and their histopathologic backgrounds. Radiographics 19 Spec No:S131-145
8. Yamashita Y, Torashima M, Takahashi M, Tanaka N, Katabuchi H, Miyazaki K, Ito M, Okamura H (1993) Hyperintense uterine leiomyoma at T2-weighted MR imaging: differentiation with dynamic enhanced MR imaging and clinical implications. Radiology 189:721–725
9. Takeuchi M, Matsuzaki K, Nishitani H (2009) Hyperintense uterine myometrial masses on T2-weighted magnetic resonance imaging: differentiation with diffusion-weighted magnetic resonance imaging. J Comput Assist Tomogr 33:834–837
10. Zaloudek C, Norris HJ (1994) Mesenchymal tumors of the uterus. In: Kurman RJ (ed) Blaustein's pathology of the female genital tract, 4th edn. New York, Springer-Verlag, pp 487–528
11. Ott D, Hennig J, Ernst T (1993) Human brain tumors: assessment with in vivo proton MR spectroscopy. Radiology 186:745–752
12. Pinker K, Stadlbauer A, Bogner W, Gruber S, Helbich TH. (2010) Molecular imaging of cancer: MR spectroscopy and beyond. Eur J Radiol. doi:10.1016/j.ejrad.2010.04.028
13. Kaji Y, Kurhanewicz J, Hricak H, Sokolov DL, Huang LR, Nelson SJ, Vigneron DB (1998) Localizing prostate cancer in the presence of postbiopsy changes on MR images: role of proton MR spectroscopic imaging. Radiology 206:785–790
14. Jung JA, Coakley FV, Vigneron DB, Swanson MG, Qayyum A, Weinberg V, Jones KD, Carroll PR, Kurhanewicz J (2004) Prostate depiction at endorectal MR spectroscopic imaging: investigation of a standardized evaluation system. Radiology 233:701–708
15. Zakian KL, Sircar K, Hricak H, Chen HN, Shukla-Dave A, Eberhardt S, Muruganandham M, Ebora L, Kattan MW, Reuter VE, Scardino PT, Koutcher JA (2005) Correlation of proton MR spectroscopic imaging with gleason score based on step-section pathologic analysis after radical prostatectomy. Radiology 234:804–814

16. Haddadin IS, McIntosh A, Meisamy S, Corum C, Styczynski Snyder AL, Powell NJ, Nelson MT, Yee D, Garwood M, Bolan PJ (2009) Metabolite quantification and high-field MRS in breast cancer. NMR Biomed 22:65–76
17. Glunde K, Jacobs MA, Bhujwalla ZM (2006) Choline metabolism in cancer: implications for diagnosis and therapy. Expert Rev Mol Diagn 6:821–829
18. Payne GS, Schmidt M, Morgan VA, Giles S, Bridges J, Ind T, DeSouza NM (2010) Evaluation of magnetic resonance diffusion and spectroscopy measurements as predictive biomarkers in stage 1 cervical cancer. Gynecol Oncol 116:246–252
19. Provencher SW (2010) LCModel & LCMgui user's manual (LCModel version 6.2-2), via http://s-provencher.com/pub/LCModel/manual/manual.pdf
20. Okada T, Harada M, Matsuzaki K, Nishitani H, Aono T (2001) Evaluation of female intrapelvic tumors by clinical proton MR spectroscopy. J Magn Reson Imaging 13:912–917
21. Celik O, Sarac K, Hascalik S, Alkan A, Mizrak B, Yologlu S (2004) Magnetic resonance spectroscopy features of uterine leiomyomas. Gynecol Obstet Invest 58:194–201
22. McLean MA, Priest AN, Joubert I, Lomas DJ, Kataoka MY, Earl H, Crawford R, Brenton JD, Griffiths JR, Sala E (2009) Metabolic characterization of primary and metastatic ovarian cancer by 1H-MRS in vivo at 3T. Magn Reson Med 62:855–861
23. Hascalik S, Celik O, Sarac K, Meydanli MM, Alkan A, Mizrak B (2005) Metabolic changes in pelvic lesions: findings at proton MR spectroscopic imaging. Gynecol Obstet Invest 60:121–127
24. Booth SJ, Pickles MD, Turnbull LW (2009) In vivo magnetic resonance spectroscopy of gynaecological tumours at 3.0 Tesla. BJOG 116:300–303
25. Stanwell P, Russell P, Carter J, Pather S, Heintze S, Mountford C (2008) Evaluation of ovarian tumors by proton magnetic resonance spectroscopy at three Tesla. Invest Radiol 43:745–751
26. Iorio E, Mezzanzanica D, Alberti P, Spadaro F, Ramoni C, D'Ascenzo S, Millimaggi D, Pavan A, Dolo V, Canevari S, Podo F (2005) Alterations of choline phospholipid metabolism in ovarian tumor progression. Cancer Res 65:9369–9376
27. Provencher SW (1993) Estimation of metabolite concentrations from localized in vivo proton NMR spectra. Magn Reson Med 30:672–679
28. Provencher SW (2001) Automatic quantitation of localized in vivo 1H spectra with LCModel. NMR Biomed 14:260–264
29. Namimoto T, Awai K, Nakaura T, Yanaga Y, Hirai T, Yamashita Y (2009) Role of diffusion-weighted imaging in the diagnosis of gynecological diseases. Eur Radiol 19:745–760
30. Takeuchi M, Matsuzaki K, Nishitani H (2009) Diffusion-weighted magnetic resonance imaging of endometrial cancer: differentiation from benign endometrial lesions and preoperative assessment of myometrial invasion. Acta Radiol 50:947–953
31. Rechichi G, Galimberti S, Signorelli M, Perego P, Valsecchi MG, Sironi S (2010) Myometrial invasion in endometrial cancer: diagnostic performance of diffusion-weighted MR imaging at 1.5-T. Eur Radiol 20:754–762
32. Fujii S, Matsusue E, Kigawa J, Sato S, Kanasaki Y, Nakanishi J, Sugihara S, Kaminou T, Terakawa N, Ogawa T (2008) Diagnostic accuracy of the apparent diffusion coefficient in differentiating benign from malignant uterine endometrial cavity lesions: initial results. Eur Radiol 18:384–389